Disentangling Cro-Magnon: The adult upper limb skeleton

Sébastien Villotte, Adrien Thibeault, Vitale Sparacello, Erik Trinkaus

Research Article

Title: Disentangling Cro-Magnon: The adult upper limb skeleton

Authors: Sébastien Villotte[1], Adrien Thibeault[2], Vitale Sparacello[2], Erik Trinkaus[3]

Affiliations: 1: PACEA, CNRS; 2: PACEA, University of Bordeaux. 3: Department of Anthropology, Washington University

Corresponding author:

Sébastien Villotte. sebastien.villotte@u-bordeaux.fr. 0033 (0)5 40 00 25 54. UMR5199 PACEA, Université de Bordeaux - CNRS. Bâtiment B8, Allée Geoffroy Saint Hilaire, CS 50023. France - 33615 PESSAC CEDEX

Key-words: Gravettian; virtual anthropology; articulating bone portions; pair matching; cortical thickness.

Abstract:

The Cro-Magnon human remains, associated with the Mid Upper Paleolithic (MUP), have been commingled since 1868. Only one comprehensive attempt to reassociate the bones and partial description of them, now more than fifty years old, has been published. This article provides a comprehensive description and reassessment of the adult upper limb remains. We used a visual and morphometric approach, combined with virtual anthropology, to allocate 14 of the 24 upper limb bones to four individuals. This analysis illustrates the relative morphological homogeneity of the MUP sample and highlights the striking differences between MUP individuals and the more recent Upper Pleistocene human groups in western Eurasia. This study also reinforces the hypothesis of gender roles during the MUP, with women more frequently than men involved in physical activities requiring both upper limbs.

Highlights:

- A multiproxy approach is used to associate the commingled Cro-Magnon upper limb bones
- Four adults are identified from the upper limb skeletal remains
- This analysis illustrates the relative morphological homogeneity of the MUP sample
- This study highlights the striking differences between MUP and LUP groups
- This study reinforces the hypothesis of gender roles during the MUP

Abbreviations:

MUP: Mid Upper Paleolithic

LUP: Late Upper Paleolithic

1. Introduction

The Cro-Magnon rock shelter (Les Eyzies-de-Tayac-Sireuil, Dordogne, France) is one of the most famous Upper Paleolithic sites in the world, best known for establishing the contemporaneity of early modern humans with Upper Paleolithic assemblages and Pleistocene fauna (Broca, 1868; Lartet, 1868). Although described in relative detail by Broca (1868) and reassessed 100 years later by Vallois and Billy (1965), the human skeletal assemblage from Cro-Magnon has remained poorly known despite the incorporation of various elements into Late Pleistocene comparative analyses. In this context, and in the framework of a broader refocus on western Eurasian Upper Paleolithic human paleobiology, we have undertaken the reassessment of the Cro-Magnon human remains (Partiot et al., 2020; Thibeault and Villotte, 2018; Villotte and Balzeau, 2018); in this contribution, we provide a description and reassessment of the upper limb remains.

The earlier Upper Paleolithic human remains from Cro-Magnon, formerly attributed generally to the "Aurignacian," are dated to the Mid Upper Paleolithic (MUP), more precisely an early phase of the Gravettian technocomplex (33–31,000 cal BP) (Henry-Gambier, 2002; Henry-Gambier et al., 2013). The relatively abundant human remains from the site are commingled, whether in situ or subsequently, resulting in various attempts to reassociate them by individual (e.g., Broca, 1968; Pruner-Bey, 1865-1875; Vallois and Billy, 1965; Henry-Gambier et al., 2013; Thibeault and Villotte, 2018; Villotte and Balzeau, 2018). Based on the cranial remains, four adults are present (Broca, 1868, Lartet, 1868, Vallois and Billy, 1965), although one of these individuals (Cro-Magnon 4) is represented only by a cranial vault piece. Gambier et al. (2006) also identified four adults from pelvic remains, but this interpretation was recently rejected (Thibeault and Villotte, 2018; see also Pruner-Bey, 1865-1875).

Using a multiproxy approach combining external morphology and virtual anthropology, the adult lower limb skeletal remains were recently allocated to three individuals (Alpha, Beta and Gamma), for whom the main biological characteristics were described (Thibeault and Villotte, 2018). Alpha was an older, tall and very robust male affected by a systemic pathological condition. Beta was an older female characterized by small long bone extremities compared to the diaphyses. Gamma was an older male, tall but much more gracile than Alpha and characterized by large long bone extremities compared to the diaphyses. There was no evidence in the lower limb skeletal assemblage of a fourth adult, in accordance with previous studies (Broca 1868; Pruner-Bey-1865-1875; Vallois and Billy 1965). These attributions raised the question of how many adults were present in the Cro-

Magnon assemblage and the whether the “Cro-Magnon 4” cranial element represented a fourth individual (Thibeault and Villotte 2018).

In this article, we therefore focus on the upper limb adult skeletal assemblage from Cro-Magnon, using a similar multiproxy approach, with four main aims:

- to provide a comprehensive description and raw data for each bone;

- to determine whether a fourth adult individual exists in the postcranial assemblage;

- to attempt to allocate the bones of the upper limb to the individuals Alpha, Beta, Gamma (or to a fourth one), in order to further elucidate their paleobiologies;

- to enhance knowledge of MUP paleobiology, and by extension behavior.

2. Material and methods

2.1. Material under study

The human remains from Cro-Magnon are curated at the Musée de l'Homme (Muséum national d'Histoire naturelle, Paris (MNHN)). This assemblage comprises twenty-four adult skeletal elements from the upper limbs (including the pectoral girdle) (Table 1).

Table 1.

2.2. Methods

2.2.1 Micro-CT data acquisition

Microtomodensitometric (µCT) data for these bones were acquired in 2017 at the AST-RX platform in the MNHN. They were obtained with the microfocus tube of the µCT scanner “v|tome|xL 240” (GE Sensing and Inspection Technologies Phoenix X ray). Each final volume was then reconstructed with isotropic voxels ranging from 89 to 144 µm and using NRecon v2.0 (Bruker microCT) in 16-bit format. Surface rendering (STL format) of these 3D models was obtained with Avizo v.9 (Visualization Sciences Group Inc.). A semi-automatic threshold-based segmentation on humeral, radial and ulnar shafts with manual corrections was carried out following the Half-Maximum Height method (Spoor et al., 1993) and by taking repeated measurements on 10 random slices of the virtual stack (Coleman and Colbert, 2007) using Avizo v.9 (Visualization Sciences Group

Inc.) and Fiji v.1.51 s (Schindelin et al., 2012). Then the endosteal and periosteal surfaces were generated on Avizo v.9 in order to produce color maps of the cortical thickness for these bones.

2.2.2. Anthropological study per bone

Identification of each element was carried out, including preservation, gross morphology, and specific features (SI-1 to SI-5). Osteometric data were collected following the Martin system (Bräuer, 1988) completed by measurements defined in Sládek et al. (2000). The morphology of the scapular axillary border was scored following Churchill (1994).

In order to estimate the maximum lengths of humeri, ulnae and radii, a well-preserved set of bones from the Upper Paleolithic was used. The SI-6 “Estimation” presents in detail the approach and the comparative sample used (see also Thibeault and Villotte, 2018). To summarize, a surface rendering of each Cro-Magnon long bone was scaled to the complete bones of five Upper Paleolithic individuals using Meshmixer 3.4 software (Autodesk, Inc.) and an averaged estimated maximum length was computed. The results are presented in Table 2.

Table 2.

2.2.3. Association of bones

In order to allocate individual bones to designated individuals, we applied the mutliproxy approach presented in detail in Thibeault and Villotte (2018) and summarized here. The zonation method (Knüsel and Outram, 2004) was used to look for overlapping in the preserved zones of fragments, and thus exclude the association of two bones from the same side. Articular congruence was checked, directly or virtually (in the latter, with Meshmixer 3.4 (Autodesk, Inc.) and MeshLab (open source) on surface rendering models, sometimes mirrored). The surface renderings of all left and right humeri, left and right ulnae, and left and right radii were superimposed virtually (mirroring one of the 3D model for each possible pair). Finally, we used color maps of the cortical thicknesses of humeral, radial and ulnar shafts (see Thibeault and Villotte, 2018) in order to assess the likelihood of an association between two elements. In order to exclude associations of bones, we also used linear regressions from maximum lengths of long bones (see Peignaux et al., 2019). Prediction intervals at a 95% threshold were generated from a large sample of modern adult individuals (Jantz and Moore-Jansen, 1988, 2000). The comparative sample, the approach used and the results obtained for Cro-Magnon remains are presented in detail in the SI-7 “Prediction interval”.

All of the data were then synthesized to establish a list of associations ordered and defined as “Impossible”, “Very unlikely”, “Possible”, “Probable” and “Almost certain” (Thibeault and Villotte, 2018). It should be noted that asymmetry (in term of size, osteometric robusticity, cross-sectional

geometry (CSG) robusticity and likely cortical distribution) of the upper limb is highly variable in the Pleistocene human sample and can be extreme for some individuals (Sparacello et al., 2017). As a result, many pairs were considered as "possible," and more value was placed on similarities in terms of discrete aspects, such as distinctive morphologies, entheseal changes and foraminal patterns.

2.2.4. Cross sectional geometry of humeri, radii and ulnae

The 3D models of the Cro-Magnon humeri, radii and ulnae were virtually positioned following Ruff (2002) when complete, and in the remaining cases the positioning and section level were approximated by comparing fragments with other MUP and Late Upper Paleolithic (LUP) virtual models with similar morphology and dimensions. Cross-sections were extracted at 50% of mechanical length (Ruff, 2002) for all bones, and additionally at 35% (mid-distal) and 80% (proximal) of mechanical length for the humerus, using Netfabb Standard 2018 for PC (© Autodesk 2017). CSG properties (cross-sectional areas and second moments of area; SI-2 to SI-4) were calculated using a version of the program SLICE (Nagurka and Hayes, 1980) adapted as a macro routine inserted in Scion Image release Beta 4.03 (Tables S4, S6 and S8).

The overall rigidity of a diaphysis reflects the baseline loads on it plus the additional loads from activity levels (Ruff 2000a, 2008); to make inferences concerning the "robusticity" of each humerus, therefore, its overall rigidity (quantified as the polar moment of area) at a given percentage of length is therefore scaled against bone (≈beam) length and estimated body mass. To provide body mass estimates for the Cro-Magnon humeri, body mass was calculated following Ruff et al. (2018) from the femoral head diameters of the lower limb individuals (Thibeault and Villotte, 2018) inferred to represent the same individuals as these humeri (see 3.2 below). Any error of association is likely to have little effect on the positions of the Cro-Magnon humeri relative to other Upper Paleolithic humeri, given the narrow range of femoral head diameters of the Cro-Magnon femora and those estimated from their acetabular diameters (Thibeault and Villotte, 2018).

2.2.5. Comparative samples

To evaluate specific traits in the Cro-Magnon sample, osteometric values were compared to samples of MUP and Late Upper Paleolithic (LUP) individuals. These samples are presented in the SI-8 "Comparative data". Data for the comparative samples are presented graphically or in the text and tables as "mean ± one standard deviation (number of individuals considered)". To compute the frequency for axillary border morphologies, when both sides were preserved and displayed the same morphology, or when only one side was preserved, the individual was counted as "1". When both sides were preserved and displayed different morphologies, "0.5" was counted for each.

3. Results and discussion

3.1. Paleobiological data per bone, and pair-matching of long bone antimeres

Data on preservation, morphology, osteometrics and cross-sectional geometry are provided for each bone in SI-1 to SI-5.

3.1.1. Pectoral girdle

There are one partial clavicle shaft and two incomplete scapulae preserved in the Cro-Magnon adult skeletal sample (SI-1; Fig. S1; Fig. 4 below). The 4290 right clavicle is one of the largest known for the western Eurasian Upper Pleistocene (Table 3). Its anteroposterior diameter at midshaft is only exceed by the MUP male Baousso da Torre 2 (left, 15.0 mm), and its circumference at midshaft only by the LUP male Marizta 2 (both sides, 52.0 mm). Its robusticity cannot be quantified due to the absence of a maximum length estimate, but it should have been substantial. The bone is characterized by a relatively round midshaft and by major entheseal changes at the deltoid attachment site (see SI-1).

Table 3

The 4291 left scapula retains only a lateral portion of the spine (SI-1; Fig. S2). The much bigger 4292 right scapula is better preserved (Fig. S2; Fig. 4 below). It is characterized by entheseal and articular degenerative changes, by four prominent foramina on the superior part of the bone and by very large dimensions. For example, the mid-axillary thickness (17.4 mm) is above the range of variation known for the MUP sample (males: 13.5 ± 1.5 (7); females: 11.4 (1)). The axillary border has strong dorsal and ventral bars. The infraglenoid tubercle continues as a sharp crest for ca. 13 mm and then fades out in the middle of the axillary border. After a small gap of ca. 7.0 mm, a rougher crest rises and continues distally to form the lateral border of the *m. teres major* attachment site, resulting in a distinctly bisulcate surface. This morphology is the most common one for the MUP, whereas it is encountered infrequently in the LUP sample (Table 4) and in recent human samples (Trinkaus 2008). The dimensions of 4291 makes it a smaller scapula than 4292, but not necessarily more gracile. These two scapulae thus appear to belong to two different individuals. Considering their similarities in terms of large dimensions and degenerative changes, the association of the 4290 right clavicle and the 4292 right scapula appears probable.

Table 4

3.1.2. Humeri

There are four adult humeri, two lefts and two rights, in the Cro-Magnon adult skeletal sample. Three of them are virtually complete, whereas the fourth one preserves only the distal shaft (SI-4; Figs. S3 to S6).

The 4294 (right) and 4295 (left) humeri are similar in term of gross morphology, shape and dimensions (SI-2; Table 5; Fig. 5 below). Their cortical distributions are also very close, and these bones display similar degenerative articular and periarticular changes. They thus form an almost certain pair, as noted by Vallois and Billy (1965). Their maximum lengths fall in the range seen for MUP females (Table 5). The only Gravettian males with humeral maximum lengths below those values are one late adolescent (Arene Candide 1) who may not have achieved full growth, and two individuals possibly (Cussac L2A) or certainly (Dolní Věstonice 15) affected by congenital systemic dysplasia. These two Cro-Magnon humeri are characterized by very small extremities, absolutely and compared to diaphyseal dimensions (Table S3; Fig. 1, Fig. 5 below). In terms of robusticity computed from external measurements, the bones appear robust compared to other Gravettian individuals (Table 6). This inference is supported by comparisons of their scaled mid-distal polar moments of area (Fig. 2), in which they fall among the most robust of the Upper Paleolithic (MUP and LUP) humeri.

Tables 5 & 6; Fig 1 and 2.

At the same time, this humeral pair does not share the extremely high asymmetry for external and CSG properties typical of Pleistocene males (Table 6; Fig. 3); its value is below the male range and exceeded in symmetry in the Upper Paleolithic sample only by the Pataud 3 female. Both 4294 and 4295 display an unusual morphology of the olecranon fossa, which seems to be subdivided into two areas (Fig. S8). They also both display a small depression at the posteromedial lateral crista of the trochlea (Fig. S8). This depression is smooth on both sides and with a normal articular surface at the bottom, but deeper and larger on the right side. The locations of the changes, centered on the lateral crista of the trochlea, and their dimensions are similar to typical trochlear osteochondritis dissecans (OCD) (Wang et al., 2019), and likely correspond to a healed condition (see Aufderheide and Rodríguez-Martin, 1998). The morphology of the changes, as well as their locations, does not correspond to sequelae of trochlear avascular necrosis, where the trochlea is misshapen and underdeveloped (Marshall et al., 2009).

Figure 3.

The third complete humerus (4293) (Figs. S3 to S7; Fig. 6 below) displays a very different morphology. Its maximum length falls in the inferior part of the Gravettian male left humeral range but outside the range of females. This left humerus is characterized by its apparent gracility

considering its large extremities, modest shaft dimensions and maximum length. The apparent gracility of the shaft, quantified by its robusticity index (16.6) is one of the lowest of the Upper Paleolithic sample, with lower values only for the Dolní Věstonice 3 and Předmostí 9 MUP females (Table 6). In addition, its mid-distal polar moment of area, scaled to length and estimated body mass, is the least robust of the Upper Paleolithic left humeri (Fig. 2). The head is extremely large in its absolute diameter compared to the Upper Paleolithic sample (Table 5) and relative to shaft dimensions (Fig. 1). The distal extremity is, to a lesser extent, also large (Table S3).

The fourth humerus (4296) is represent by the distal third of the diaphysis (SI-2). 4296 appears fairly robust. The supracondylar antero-posterior diameter for this bone is the largest of the Upper Paleolithic sample. Its minimum distal perimeter (68.0 mm) is well above the means computed for the comparative samples (Table 6). Although its percent cortical area (79.6%) is similar to the other Cro-Magnon humeri (Table S4; Fig. S9), its polar moment of area is well above those of the other Cro-Magnon 35% sections (Table S4). Based on external morphology, CSG properties at 35%, as well as cortical bone distribution, 4296 does not make an obvious pair with 4293; a 35% polar moment of area asymmetry value for 4296 and 4293 is 207.5%, which is completely outside the range of even the relatively asymmetrical Upper Paleolithic paired humeri (Sparacello et al., 2017; Fig. 3).

Tables 5 and 6

3.1.3 Ulnae

The ulna is the best represented bone in the Cro-Magnon adult upper limb skeletal assemblage (Table 1; SI-3; Figs. S10 to S13). It thus represents the best bone for assessing the minimum number of individuals (MNI). There are six ulnar pieces, four lefts and two rights. The analysis of both the actual bones and their 3D models indicates that the four left fragments overlap (Figs. S10 to S13; Fig. 7 below), demonstrating a minimum number of individuals of four adults for the upper limb skeletal assemblage. Two individuals are each represented by a pair (4300 and 4302; 4297 and 4298) and two individuals are represented by a singleton (the left ulnae 4299 and 4301).

The 4299 left ulna is preserved from the proximal olecranon to the proximal end of the *m. pronator quadratus* tuberosity. Its distal end is covered by concretions. Its estimated maximum length falls in the upper part of the range seen for MUP males (Table 7). The diaphysis of the bone displays high dimensions and is very robust (Table 8). Its proximal end is the largest of the UP sample (Table 7), only equaled by the MUP male Pavlov 1 for the olecranon breadth. A very thick enthesophyte is present at the posterior margin of the *m. triceps brachii* attachment site, and the

margin of the trochlear notch and the radial facet displays osteophytic lipping and localized bone outgrowths (Fig. S15).

Tables 7 & 8

4301 is a left ulna preserved from the proximal olecranon to midshaft (Fig. 5 below). This bone clearly separates from the other ulnae by its small maximum length and proximal extremity dimensions (Table 7). It does not exhibit any significant characteristics, apart a relatively smaller proximal extremity than the other ulnae (Table 7; SI-3).

The 4300 right ulna and the 4302 left ulna are both represented by the proximal third of the bone (SI-3; Fig. 6 below). They form a probable pair, based on their similarity in gross morphology (size and shape of the coronoid process and the radial articular facet, size and shape and orientation of the olecranon), presence of foramina, and articular and entheseal changes. The superposition of the left bone on the mirrored right one fits very well. Their maximum lengths fall in the upper part of the range of variation seen MUP males (Table 7). Their olecranon dimensions are large compared to other individuals, especially for the right bone (Table 7). A well-developed enthesophyte is present at the posterior margin of the *m. triceps brachii* attachment site of both bones (Figs. S16 and S17). Minor osteoarthrosic changes (i.e. osteophytic lipping associated with foramina) are present at the margin of the trochlear notch of both bones (SI-3).

The 4297 right ulna is the most complete of the assemblage, but it is heavily reconstructed. The study of its gross morphology allowed us to identify a poor reconstruction at mid shaft (SI-3; Figs. S10; Fig. 7 below). A virtual reconstruction of this bone, based on 3D models of each of its fragments, was therefore carried out (SI-3; Fig. S14). The 4297 maximum length was initially considered to be ca. 295 mm. After reconstruction, this measure appears closer to 290 (Table 2), but it still remains in the upper part of the range of variation seen for MUP males and outside the range computed for other sub samples (Table 7). The other linear measurements indicate a moderately robust bone (Tables 7 and 8).

The 4298 left ulna is preserved from the proximal interosseous crest to the distal end. 4298 and 4297 form a probable pair, based on the same location of the nutrient foramen, the presence of a sulcus between the interosseous crest and the posterior border at midshaft for both bones, the similar curvatures of the bones, and the presence in both cases of two foramina and a depression between the distal articular surface and the styloid process (SI-3).

Tables 7 and 8

3.1.4. Radii

Five radii are present in adult skeletal assemblage, three lefts and two rights (SI-4; Figs. S19 to S22). There is no clear pair-matching for these bones. The estimated maximum lengths of 4303, 4304, 4306 and 4307 fall in the middle of the range of variation known for MUP males (Table 9). The maximum length of 4305 cannot be securely estimated, but it appears that this bone is the shortest radius of the assemblage (Fig. S19).

The 4303 left radius is preserved from the head to the distal flare (Fig. 6 below). Whereas its diaphyseal dimensions are not especially large (Table 10), its head, which is evenly concave proximally, is very large: its estimated maximum diameter of ca. 25.9 mm is only exceed by Barma Grande 2 (a MUP male). The 4305 left radius is preserved from the head to midshaft (Fig. 5 below). This bone is characterized by an evenly rounded and rather small head (Table 9), especially compared to its shaft dimensions (Table 10).

The 4307 left radius (preserved from the distal radial tuberosity to the mid-distal diaphysis) is the more substantial left radius of the whole UP sample (Table 10). The values for its antero-posterior and medio-lateral diameters at the maximum development of crest are the highest of the whole UP sample, and the minimum perimeter of its shaft is only equaled for the left side by Barma Grande 2 (Table 10). The 4304 right radius (Fig. 4 below), preserved from the beginning of the interosseous crest proximally to the broken trabeculae of the distal epiphysis, also appears very robust with very large dimensions (Table 10). For instance, its value for the minimum perimeter is exceeded only for the right side by Baousso da Torre 1 and Barma Grande 2 (two MUP males). This bone is also characterized by an antero-posteriorly thick interosseous crest, a marked area for the attachment of *m. pronator teres* with a raised area through its longitudinal middle, and very prominent dorsal tubercles. Its association with 4303 is very unlikely due to too many differences in term of size and shape. Its association with 4305 or 4307 is possible. The 4306 right radius is represented by the diaphysis and the distal end. The bone appears relatively gracile compared to the other ones. It may be the antimere of 4303, but this association remains only possible.

Tables 9 and 10.

3.1.5. Hand bones

There are three metacarpals and three hand phalanges in the adult skeletal assemblage (SI-5; Figs. S24 and S25). There is little to note in term of morphology for these bones. Primarily the metacarpals show little accentuation of the interosseus muscle origins and the flexor sheath crests on the proximal phalanges are modest.

The partial second and the complete third left metacarpals (4308 and 4309) probably belong to the same individual, based on similarities in term of morphology, size, minor pathological changes and color of the bones. The 4310 fourth right metacarpal is too long to belong to the same individual as 4309. The third left (4311) and right (4312) proximal phalanges are likely not from the same individual. They differ in term of morphology and size. The size and morphology of 4313 (a right second proximal phalanx) is compatible with 4312.

3.2. Allocations of bones to individuals, and individual characteristics

Based on the ulnae, four adults are represented in the upper limb skeletal assemblage. Fortunately, the ulnae are different enough to 1) associate them to previously described individuals Alpha, Beta and Gamma, and 2) to identify some specificities for the fourth individual, called Delta.

3.6.1. Individual Alpha (Fig. 4)

The 4299 left ulna can be allocated with certainty to individual Alpha. Its impressive dimensions, associated with major articular and entheseal changes, and the presence of concretions are all indicative of an allocation to this individual. This bone does not articulate well (virtually or directly) with the preserved distal extremities of the three complete humeri. Considering the impressive dimensions and the degenerative changes of the 4290 right clavicle, the 4292 right scapula, and the 4304 right radius, these bones are considered as probably belonging to Alpha.

It is also probable that the 4296 distal humeral shaft belongs to either Alpha or Delta (see below). Its diaphyseal dimensions are considerably larger than those of the other Cro-Magnon humeri (see above), and they would be in agreement with the large dimensions of Alpha's other upper limb remains. However, the paired ulnae of Delta are also large, which makes the attribution of 4296 to Alpha tentative.

Figure 4

3.6.2. Individual Beta (Fig. 5)

The female Beta is characterized by relatively short and robust bones, and very small extremities compared to shaft dimensions. Several bones in upper limb adult skeletal assemblage fit with this morphology: the 4294 and 4295 pair of humeri, the 4301 left ulna, and the 4305 left radius. This association is confirmed by the estimated maximum lengths (SI-7): the humeri are too short to be associated with any other ulna or radius. Moreover, the olecranon margin of the 4301 left ulna fits perfectly with the unusual morphology of the olecranon fossa of 4295.

Beta's upper limb bones are relatively robust with a very low asymmetry, which is consistent with previous results regarding Upper Pleistocene females (Sparacello et al., 2017). As with her lower limb remains, degenerative changes are present, but relatively moderate, on the upper limb bones of Beta. This individual also displays healed OCD of the humeral trochlea bilaterally (but more marked at the right side). OCD of the humeral trochlea is very rare currently (Wang et al. 2019, Marshall et al. 2019) and typically affects adolescent athletes (of both sexes) with open physes (Wang et al. 2019). It has been hypothesized that trochlear OCD lesions is mechanically induced at a time of vascular vulnerability when the capitular ossification center is about to fuse with the trochlear ossification center (Wang et al. 2019).

Figure 5

3.2.3. Individual Gamma (Fig. 6)

The individual Gamma is characterized by moderately robust bones with very large extremities. The 4293 left humerus, the 4300 and 4302 pair of ulnae, and the 4303 left radius display this distinctive morphology. Moreover, the 3D model of 4302 and the mirrored 3D model of 4300 articulate well with the 4293 left humerus; and the 4303 radius articulates well with the 4302 ulna.

Figure 6

3.2.4. Individual Delta (Fig. 7)

The fourth adult, which was not identified in the lower limb skeletal assemblage, is called Delta. This individual is defined by the 4297 and 4298 pair of ulnae. As only two bones are securely referred to this individual, it is not possible to provide an accurate biological profile for him/her. Nevertheless, a few comments can be pointed out. Firstly, contrary to Alpha, Delta does not seem to be characterized by major degenerative changes. Secondly, the dimensions of the 4297 and 4298 ulnae appear very high. Delta was likely a very tall individual, almost certainly taller than Beta and Gamma. Thirdly, the ulnae are not characterized by either small or big epiphyses compared to their shafts. This clearly distinguishes Delta from individuals Beta and Gamma. It remains unclear whether the 4296 distal humeral shaft belongs to Alpha or Delta, but assuming that there is not a fifth adult present among the Cro-Magnon adult remains, it should belong to one of them.

Figure 7

3.2.5. Hand bone allocation

The six metacarpals and proximal phalanges cannot be securely associated with any of these four adults, given substantial variation in hand to arm bone lengths. However, the modest muscle

attachments and minimal periarticular changes of these hand bones suggest that they do not belong to Alpha.

3.2.6. Summary

Due to both the high levels of asymmetry commonly encountered for Pleistocene upper limb remains, and the fourth individual evident in the ulnae, we were cautious in the pair matching and allocation of the other bones to a given individual. As a result, only 14 (out of 24) bones were associated with one of the adults (Table 11). Nevertheless, our analysis permitted the allocation of more bones to identified individuals than previous studies, including the principal one carried out by Vallois and Billy (1965). Moreover, our associations are very different from those proposed by those authors. For instance, all the "gracile" bones were allocated to Cro-Magnon 2 in their study. These bones (e.g. 4293 and 4303) are however characterized by very large extremities and large maximum lengths and these characteristics are clearly incompatible with the only female coxal bone 4317, which is rather small and with a small acetabulum.

Table 11

3.3. Implications for western Eurasian population history and MUP lifestyle

This analysis of the adult upper limb remains from Cro-Magnon indicates that the individuals from this site do not particularly distinguish them from other MUP individuals. Some of the skeletal elements, especially those associated with individual Alpha, are among the biggest (and sometimes the biggest) upper limb bones of the whole Upper Paleolithic sample. This places the Cro-Magnon sample close to MUP sites from Liguria, where extremely tall and robust individuals were buried (Formicola and Holt, 2015; Rivière, 1887; Verneau, 1906; Villotte et al., 2017). This analysis thus illustrates the relative morphological homogeneity of the MUP sample (spread through western Eurasia and for ca. 10 000 years) and highlights the striking differences between MUP individuals and LUP individuals. This is especially clear for long bone maximum lengths and for the scapular axillary border.

The Cro-Magnon individuals, as well as other subjects from the MUP, tend to have longer bones than LUP individuals. This has been noticed for a long time (Formicola and Giannecchini, 1999; Jacobs, 1985) and interpreted as a reduction in gene flow and decline in nutritional conditions between the MUP and the LUP. However, based on recent paleogenomic studies (Fu et al., 2016; Posth et al., 2016), the differences between MUP and LUP skeletal morphology seems more likely related to a turnover of population across the Late Glacial Maximum. The same hypothesis can be

formulated for the scapular axillary border morphology. While the dominance of the scapular dorsal axillary border morphology among the Neandertals and its implications has been a focus for more than a century (Boule, 1911-1913; Churchill, 1994; Di Vincenzo et al., 2019; Odwak, 2006; Trinkaus, 2015, 2008a, 2008b, 1977; von Eickstedt, 1925), little attention has been paid to the chronological differences within the Upper Paleolithic. To our knowledge, only one article (Trinkaus, 2015) distinguished the MUP and LUP subsamples and thus identified the striking differences in terms of frequencies of scapular axillary borders between these two groups. The functional significance of variation in scapular axillary border morphology remains unclear, while comparative adult analyses (Churchill, 1994; Odwak, 2006; Trinkaus, 2008b) and developmental assessments (Trinkaus, 2008a; Trinkaus et al., 2014) suggests a genetic basis to variation in axillary morphology within and between groups.

Due to the very few probable pair matching identified in this sample, inferences on MUP behaviors are limited. However, some remarks are possible for individual Beta. Upper limb bones of this woman are relatively robust, with a very low asymmetry, which is consistent with previous results regarding Late Pleistocene females (Sparacello et al., 2017). Low levels of asymmetry can be the product of either general gracility or bilateral hypertrophy from bi-manual activities (Ogilvie and Hilton, 2011; Shaw and Stock, 2009), the latter being the more probable case for Late Pleistocene individuals in general (see Sparacello et al., 2017) and for Beta in particular. This interpretation is in agreement with her bilateral OCD of the humeral trochleae. Considering the probable etiology of trochlear OCD, it seems indeed likely that these lesions, as well as the overall robusticty of Beta's upper limbs, are related to the intensive use of both upper limbs during the growth of this individual. If one considers the slight degenerative changes seen at joints and entheses as related to mechanical solicitations, the low asymmetry in term of location and intensity of these lesions may indicate that this bimanual activities were still common during the adult life of Beta. However, considering the advanced age at death of this individual, it is also possible that the changes were part of a systemic degenerative processes related to senescence (Villotte et al., 2010a; Villotte and Knüsel, 2013). In either case, the paleobiological assessment of Beta's upper limbs supports the hypothesis of sexual division of labor(s) in western Eurasian Upper Pleistocene groups, with women apparently more commonly involved in strenuous bi-manual activities and/or more diverse activities than men (Sparacello et al., 2017; Villotte et al., 2017, 2010b), a pattern also frequently highlighted during the Holocene (e.g. Macintosh et al., 2017; Sparacello et al., 2011; Villotte and Knüsel, 2014).

Conclusions

Since their discovery, the adult upper limb remains from Cro-Magnon have attracted little interest within the paleoanthropological community (Villotte and Balzeau 2018), likely due to the difficulty to identify pairs and to allocate them to designated individuals. We provide in this article a comprehensive paleobiological assessment of each bone of the upper limb adult skeletal assemblage and allocated 14 of them to one of the four identified adult individuals. One of them, individual Delta, was not previously identified and is now defined by a pair of ulnae.

This study emphasizes the relative morphological homogeneity of the MUP western Eurasian sample, suggesting exogamy and regular exchanges between small reproductive groups, as well as the striking differences between this sample and the more recent Late Pleistocene human groups that lived in western Eurasia, likely related to a turnover of population across the Late Glacial Maximum. This study also reinforce the hypothesis of specific social roles associated to males and females (i.e. genders) during the MUP, with women involved in strenuous, diverse, and/or bi-manual activities, whereas men may have been more associated to uni-manual tasks. Such gendered activities remain to be identified.

Acknowledgements

The authors thank Veronique Laborde, Aurélie Fort (curators at the Musée de l'Homme) and Dominique Grimaud-Hervé (in charge of the collection) for granting access to the Cro-Magnon remains. We are grateful to Dominique Henry-Gambier for sharing her knowledge about the Cro-Magnon site and human remains, and to the many colleagues who shared data on Upper Paleolithic skeletons. We would like to thank Dr. Richard Jantz for making the Forensic Databank data available.

Funding sources

The research is a part of the project Gravett'Os funded by the Agence Nationale de la Recherche (Grant number: ANR-15-CE33-0004).

Competing interests

The authors declare that they have no conflict of interest.

References cited

Boule, M., 1911-1913. L'homme fossile de La Chapelle-aux-Saints, Annales de Paléontologie. ed. Paris.

Bräuer, G., 1988. Osteometrie, in: Knussmann, R. (Ed.), Anthropologie: Handbuch Der Vergleichenden Biologie Des Menschen. G. Fischer, Stuttgart, pp. 160–232.
Broca, P., 1868. Sur les crânes et ossements des Eyzies. Bulletins de la Société d'Anthropologie de Paris 3, 350–392.
Churchill, S.E., 1994. Human upper body evolution in the Eurasian later Pleistocene.
Coleman, M.N., Colbert, M.W., 2007. Technical note: CT thresholding protocols for taking measurements on three-dimensional models. American Journal of Physical Anthropology 133, 723–725. https://doi.org/10.1002/ajpa.20583
Di Vincenzo, F., Churchill, S.E., Buzi, C., Profico, A., Tafuri, M.A., Micheli, M., Caramelli, D., Manzi, G., 2019. Distinct among Neanderthals: The scapula of the skeleton from Altamura, Italy. Quaternary Science Reviews 217, 76–88. https://doi.org/10.1016/j.quascirev.2018.11.023
Formicola, V., Giannecchini, M., 1999. Evolutionary trends of stature in Upper Paleolithic and Mesolithic Europe. Journal of Human Evolution 36, 319–333. https://doi.org/10.1006/jhev.1998.0270
Formicola, V., Holt, B.M., 2015. Tall guys and fat ladies: Grimaldi's Upper Paleolithic burials and figurines in an historical perspective. J Anthropol Sci. 93, 71–88.
Fu, Q., Posth, C., Hajdinjak, M., Petr, M., Mallick, S., Fernandes, D., Furtwängler, A., Haak, W., Meyer, M., Mittnik, A., Nickel, B., Peltzer, A., Rohland, N., Slon, V., Talamo, S., Lazaridis, I., Lipson, M., Mathieson, I., Schiffels, S., Skoglund, P., Derevianko, A.P., Drozdov, N., Slavinsky, V., Tsybankov, A., Cremonesi, R.G., Mallegni, F., Gély, B., Vacca, E., Morales, M.R.G., Straus, L.G., Neugebauer-Maresch, C., Teschler-Nicola, M., Constantin, S., Moldovan, O.T., Benazzi, S., Peresani, M., Coppola, D., Lari, M., Ricci, S., Ronchitelli, A., Valentin, F., Thevenet, C., Wehrberger, K., Grigorescu, D., Rougier, H., Crevecoeur, I., Flas, D., Semal, P., Mannino, M.A., Cupillard, C., Bocherens, H., Conard, N.J., Harvati, K., Moiseyev, V., Drucker, D.G., Svoboda, J., Richards, M.P., Caramelli, D., Pinhasi, R., Kelso, J., Patterson, N., Krause, J., Pääbo, S., Reich, D., 2016. The genetic history of Ice Age Europe. Nature 534, 200–205. https://doi.org/10.1038/nature17993
Gambier, D., Bruzek, J., Schmitt, A., Houët, F., Murail, P., 2006. Révision du sexe et de l'âge au décès des fossiles de Cro-Magnon (Dordogne, France) à partir de l'os coxal. Comptes Rendus Palevol 5, 735–741. https://doi.org/10.1016/j.crpv.2005.12.011
Henry-Gambier, D., 2002. Les fossiles de Cro-Magnon (Les eyzies-de-Tayac, Dordogne) : nouvelles données sur leur position chronologique et leur attribution culturelle. Bulletins et Mémoires de la Société d'Anthropologie de Paris n.s., 14, 89–112.
Henry-Gambier, D., Nespoulet, R., Chiotti, L., 2013. An Early Gravettian cultural attribution for the human fossils from the Cro-Magnon rock shelter (Les Eyzies-de-Tayac, Dordogne). Paleo 24, 121–138.
Jacobs, K.H., 1985. Evolution in the postcranial skeleton of Late Glacial and early Postglacial European hominids 307–326.
Jantz, R., Moore-Jansen, P., 1988. A data base for forensic anthropology. Washington, DC USA: Final Report to the National Institute of Justice.
Jantz, R.J., Moore-Jansen, P.H., 2000. Database for Forensic Anthropology in the United States, 1962-1991. Inter-university Consortium for Political and Social Research.
Knüsel, C.J., Outram, A., 2004. Fragmentation: The Zonation Method Applied to Fragmented Human Remains from Archaeological and Forensic Contexts. Environmental Archaeology 9, 85–98.
Lartet, L., 1868. Une sépulture des troglodytes du Périgord (crânes des Eyzies). Bulletins de la Société d'anthropologie de Paris 3, 335–349. https://doi.org/10.3406/bmsap.1868.9547
Macintosh, A.A., Pinhasi, R., Stock, J.T., 2017. Prehistoric women's manual labor exceeded that of athletes through the first 5500 years of farming in Central Europe. Science Advances 3, eaao3893. https://doi.org/10.1126/sciadv.aao3893
Nagurka, M., Hayes, W., 1980. An interactive graphics package for calculating cross-sectional properties of complex shapes. J. Biomech 13, 59–64.

Odwak, H., 2006. Scapular Axillary Border Morphology in Modern Humans and Neandertals. Period biol 108, 12.
Ogilvie, M.D., Hilton, C.E., 2011. Cross-sectional geometry in the humeri of foragers and farmers from the prehispanic American Southwest: Exploring patterns in the sexual division of labor. American Journal of Physical Anthropology 144, 11–21. https://doi.org/10.1002/ajpa.21362
Partiot, C., Trinkaus, E., Knüsel, C.J., Villotte, S., 2020. The Cro-Magnon babies: Morphology and mortuary implications of the Cro-Magnon immature remains. Journal of Archaeological Science: Reports 30, 102257. https://doi.org/10.1016/j.jasrep.2020.102257
Peignaux, C., Kacki, S., Guyomarc'h, P., Schotsmans, E.M.J., Villotte, S., 2019. New anthropological data from Cussac Cave (Gravettian, Dordogne, France): In situ and virtual analyses of Locus 3. Comptes Rendus Palevol 18, 455–464. https://doi.org/10.1016/j.crpv.2019.02.004
Posth, C., Renaud, G., Mittnik, A., Drucker, D.G., Rougier, H., Cupillard, C., Valentin, F., Thevenet, C., Furtwängler, A., Wißing, C., Francken, M., Malina, M., Bolus, M., Lari, M., Gigli, E., Capecchi, G., Crevecoeur, I., Beauval, C., Flas, D., Germonpré, M., van der Plicht, J., Cottiaux, R., Gély, B., Ronchitelli, A., Wehrberger, K., Grigorescu, D., Svoboda, J., Semal, P., Caramelli, D., Bocherens, H., Harvati, K., Conard, N.J., Haak, W., Powell, A., Krause, J., 2016. Pleistocene Mitochondrial Genomes Suggest a Single Major Dispersal of Non-Africans and a Late Glacial Population Turnover in Europe. Current Biology 26, 827–833. https://doi.org/10.1016/j.cub.2016.01.037
Pruner-Bey, F., 1865–1875. An account of the human bones found in the cave of Cro-Magnon in Dordogne. In: Lartet, E., Christy, H. (Eds.), Reliquiae Aquitanicae: being Contributions to Anthropology and Palaeontology of Périgord and the Adjoining Provinces of Southern France. Vol. 1. William and Morgate, London, pp. 73–92.
Rivière, E., 1887. Antiquité de l'homme dans les Alpes-Maritimes. J.-B. Baillière, Paris.
Ruff, C., 2002. Variation in Human Body Size and Shape. Annual Review of Anthropology 31, 211–232. https://doi.org/10.1146/annurev.anthro.31.040402.085407
Ruff, C.B., Burgess, M.L., Squyres, N., Junno, J.A., Trinkaus, E. (2018) Lower limb articular scaling and body mass estimation in Pliocene and Pleistocene humans. *Journal of Human Evolution* 115: 85-111. https//doi.10.1016/j.jhevol.2017.10.014.
Schindelin, J., Arganda-Carreras, I., Frise, E., Kaynig, V., Longair, M., Pietzsch, T., Preibisch, S., Rueden, C., Saalfeld, S., Schmid, B., Tinevez, J.-Y., White, D.J., Hartenstein, V., Eliceiri, K., Tomancak, P., Cardona, A., 2012. Fiji: an open-source platform for biological-image analysis. Nature Methods 9, 676. https://doi.org/10.1038/nmeth.2019
Shaw, C.N., Stock, J.T., 2009. Habitual throwing and swimming correspond with upper limb diaphyseal strength and shape in modern human athletes. American Journal of Physical Anthropology 140, 160–172. https://doi.org/10.1002/ajpa.21063
Sládek, V., Trinkaus, E., Hillson, S.W., Holliday, T.W., 2000. The people of the Pavlovian. Skeletal catalogue and osteometrics of the Gravettian fossil hominids from Dolní Věstonice and Pavlov. Academy of Sciences of the Czech Republic, Brno.
Sparacello, V.S., Pearson, O.M., Coppa, A., Marchi, D., 2011. Changes in skeletal robusticity in an iron age agropastoral group: The samnites from the Alfedena necropolis (Abruzzo, Central Italy). American Journal of Physical Anthropology 144, 119–130. https://doi.org/10.1002/ajpa.21377
Sparacello, V.S., Villotte, S., Shackelford, L.L., Trinkaus, E., 2017. Patterns of humeral asymmetry among Late Pleistocene humans. Comptes Rendus Palevol 16, 680–689. https://doi.org/10.1016/j.crpv.2016.09.001
Spoor, C.F., Zonneveld, F.W., Macho, G.A., 1993. Linear measurements of cortical bone and dental enamel by computed tomography: Applications and problems. American Journal of Physical Anthropology 91, 469–484. https://doi.org/10.1002/ajpa.1330910405

Thibeault, A., Villotte, S., 2018. Disentangling Cro-Magnon: A multiproxy approach to reassociate lower limb skeletal remains and to determine the biological profiles of the adult individuals. Journal of Archaeological Science: Reports 21, 76–86.
Trinkaus, E., 2015. The appendicular skeletal remains of Oberkassel 1 and 2, in: Giemsch, L., Schmitz, R.W. (Eds.), The Late Glacial Burial from Oberkassel Revisited. Verlag Phillip von Zabern, Darmstadt, pp. 75–132.
Trinkaus, E., 2008a. Kiik-Koba 2 and Neandertal axillary border ontogeny. Anthropological Science 116, 231–236. https://doi.org/10.1537/ase.071221
Trinkaus, E., 2008b. Behavioral implications of the Muierii 1 early modern human scapula. Annuaire Roumain d'Anthropologie 45, 27–41.
Trinkaus, E., 1977. A functional interpretation of the axillary border of the Neandertal scapula. Journal of Human Evolution 6, 231–234. https://doi.org/10.1016/S0047-2484(77)80047-X
Trinkaus, E., Buzhilova, A.P., Mednikova, M.B., Dobrovolskaya, M.V., 2014. The People of Sunghir. Burials, Bodies, and Behavior in the Earlier Upper Paleolithic. Oxford University Press, New York.
Vallois, H.V., Billy, G., 1965. Nouvelles recherches sur les hommes fossiles de l'abri de Cro-Magnon. L'Anthropologie 69, 47–74.
Verneau, R., 1906. Les grottes de Grimaldi (Baoussé-Roussé), Anthropologie, II-1. Imprimerie de Monaco, Monaco.
Villotte, S., Balzeau, A., 2018. Que reste-t-il des Hommes de Cro-Magnon 150 ans après leur découverte ? BMSAP 30, 146–152. https://doi.org/10.3166/bmsap-2018-0026
Villotte, S., Castex, D., Couallier, V., Dutour, O., Knüsel, C.J., Henry-Gambier, D., 2010a. Enthesopathies as occupational stress markers: evidence from the upper limb. American Journal of Physical Anthropology 142, 224–234.
Villotte, S., Churchill, S.E., Dutour, O., Henry-Gambier, D., 2010b. Subsistence activities and the sexual division of labor in the European Upper Paleolithic and Mesolithic: evidence from upper limb enthesopathies. Journal of Human Evolution 59, 35–43.
Villotte, S., Knüsel, C.J., 2014. "I sing of arms and of a man…": medial epicondylosis and the sexual division of labour in prehistoric Europe. Journal of Archaeological Science 43, 168–174. https://doi.org/10.1016/j.jas.2013.12.009
Villotte, S., Knüsel, C.J., 2013. Understanding Entheseal Changes: Definition and Life Course Changes. International Journal of Osteoarchaeology 23, 135–146. https://doi.org/10.1002/oa.2289
Villotte, S., Samsel, M., Sparacello, V., 2017. The paleobiology of two adult skeletons from Baousso da Torre (Bausu da Ture) (Liguria, Italy): Implications for Gravettian lifestyle. Comptes Rendus Palevol 16, 462–473. https://doi.org/10.1016/j.crpv.2016.09.004
von Eickstedt, E.F., 1925. Variationen am Axillarrand der Scapula. Anthropologischer Anzeiger, 2, 217–228.

Tables

Table 1. Adult skeletal elements from the upper limbs at Cro-Magnon

MNHN code	Bone	Preservation
4290	Right clavicle	Lateral half of the diaphysis
4291	Left scapula	Spine

4292	Right scapula	Spine, lateral axillary border and glenoid cavity
4293	Left humerus	Complete
4294	Right humerus	Complete
4295	Left humerus	Complete
4296	Right humerus	Distal half of the diaphysis
4297	Right ulna	Complete (reconstructed)
4298	Left ulna	Distal half of the bone
4299	Left ulna	Proximal two thirds of the bone
4300	Right ulna	Proximal third of the bone
4301	Left ulna	Proximal half of the bone
4302	Left ulna	Proximal third of the bone
4303	Left radius	Distal extremity missing
4304	Right radius	Head, radial tuberosty and distal extremity missing
4305	Left radius	Proximal half of the bone
4306	Right radius	Distal two thirds of the bone
4307	Left radius	Diaphysis
4308	Left Metacarpal II	Distal half of the metacarpal
4309	Left metacarpal III	Complete
4310	Right metacarpal IV	Complete
4311	Left proximal phalanx III	Complete
4312	Right proximal phalanx III	Complete
4313	Right proximal phalanx II	Complete

Table 2. Estimations of maximum length of the long bones of the upper limb. Measurements are in millimeters. *: after virtual reconstruction.

Code	Bone	Average estimated maximum length	Standard deviation	Coefficient of variation	Minimal estimation	Maximal estimation
4297	R. Ulna*	289.7	0.8	0.3%	288.9	291.0
4298	L. Ulna	290.2	3.0	1.0%	286.7	294.7
4299	L. Ulna	296.9	1.7	0.6%	294.6	298.9
4300	R. Ulna	293.8	3.4	1.2%	289.3	297.4
4301	L. Ulna	269.1	2.8	1.0%	266.5	273.7
4302	L. Ulna	290.7	2.9	1.0%	288.4	295.3
4303	L. Radius	267.0	4.5	1.7%	261.8	273.0
4304	R. Radius	269.7	0.8	0.3%	268.7	270.5
4307	L. Radius	267.3	2.9	1.1%	264.2	271.6

Table 3. Clavicular midshaft dimensions. Measurements are in millimeters.

		Mid. S-I Diameter (M4)		Mid. A-P Diameter (M5)		Mid. Circumference (M6)	
		Right	Left	Right	Left	Right	Left
Cro-Magnon	4290	13.2		14.1		45	
Neandertal	Females						
	Males						
MUP	Females	9.7 ± 1.4 (5)	9.9 ± 2.4 (5)	10.5 ± 1.7 (5)	10.6 ± 1.3 (5)	34.4 ± 3.2 (5)	35 ± 3.9 (5)
	Males	12.2 ± 0.9 (8)	11.6 ± 1 (8)	12.2 ± 1.1 (8)	12.4 ± 1.5 (8)	40.4 ± 1.9 (8)	38.4 ± 2.7 (8)
LUP	Females	9.6 ± 1.4 (5)	9.5 ± 2.1 (5)	9.9 ± 0.6 (5)	9.5 ± 0.7 (5)	31.3 ± 4 (5)	29 ± 4.2 (5)
	Males	10.4 ± 2.2 (13)	10 ± 2.8 (13)	11.2 ± 1.1 (13)	10.8 ± 0.8 (13)	35.8 ± 4.6 (13)	33.8 ± 4.1 (13)

Table 4. Comparative frequencies of axillary border morphology. CM not included. An individual with the same morphology on both sides or with only one side preserved was computed as “1” for a given category, whereas an individual with bilateral asymmetry was computed as “0.5” for each morphology.

	Ventral sulcus	Bisulcate	Dorsal sulcus	N
Neandertals	1.8%	23.2%	75.0%	28
MUP	16.7%	66.7%	16.7%	24
LUP	81.6%	18.4%	0.0%	19

Table 5. Humeral maximum length and proximal and distal dimensions

		Max. Length (M1)	Prox. Epic. Breadth (M3)	Head sagittal Diam. (M10)	Dist. Epic. Breadth (M4)
Cro-Magnon	4294 (right)	321.0	45.0	43.4	56.0
	4295 (left)	323.0			56.0
	4293 (left)	337.0		50.2	62.5
	4296 (right)				
MUP	Females	318.4 ± 16.1 (7)	49.2 ± 1.1 (5)	47.3 ± 1.8 (4)	58.3 ± 3.3 (6)
	Males	342.7 ± 26.2 (17)	51.8 ± 2 (9)	48.6 ± 2.4 (11)	62.7 ± 4.4 (15)
LUP	Females	287.9 ± 17.6 (6)	45.5 ± 1.6 (5)	42 ± 1.2 (3)	53.2 ± 2.8 (6)
	Males	308.4 ± 15.3 (13)	48.9 ± 2.4 (11)	47.5 ± 2.8 (10)	60.5 ± 3.2 (16)

Table 6. Humeral shaft dimensions and robusticity. Measurements are in millimeters.

		Dist. Min. Circumference (M7)		Classical robusticity	
		Right	Left	Right	Left
Cro-Magnon	4294 and 4295	64.0	63.0	19.9	19.5
	4293		56.0		16.6
	4296	68.0			
MUP	Females	58.6 ± 4.3 (5)	56.3 ± 4.3 (6)	18.6 ± 0.6 (4)	17.8 ± 1.7 (5)
	Males	67.1 ± 5.3 (15)	61.1 ± 3.3 (18)	19.1 ± 1 (12)	17.8 ± 0.7 (13)
LUP	Females	55.7 ± 4.7 (6)	53.8 ± 5.3 (7)	19.4 ± 0.7 (4)	19.1 ± 1.3 (5)
	Males	64.8 ± 3.3 (16)	60.7 ± 6.2 (15)	20.7 ± 0.8 (12)	19.3 ± 1.8 (10)

Table 7. Ulnar maximum length and proximal dimensions

		Maximum Length M1	Olecranon Length M8	Olecranon Breadth M6	Olecranon depth M7
Cro Magnon	4297 (right)	289.7	23.4	27.3	25
	4298 (left)	290.2			
	4299 (left)	296.9	26.5	31	29
	4300 (right)	293.8	23.7	27.5	28.2
	4301 (left)	269.1	21.6		24.5
	4302 (left)	290.7	23.4		25.5
MUP	Females	266.4 ± 14.4 (6)	16.9 ± 3.6 (3)	22.5 ± 3.5 (3)	22.9 ± 2.5 (3)
	Males	284.1 ± 18.3 (10)	20.6 ± 1.7 (13)	26.8 ± 2.2 (13)	25.2 ± 1 (13)
LUP	Females	237.9 ± 14.8 (7)	19 ± 1.3 (3)	23.1 ± 2.9 (5)	23.4 ± 1 (3)
	Males	256.1 ± 16.1 (14)	21.7 ± 1.8 (6)	24.9 ± 1.1 (9)	24.7 ± 2 (7)

Table 8. Ulnar shaft dimensions and robusticity

		Crest A-P diameter M11		Crest M-L diameter M12		Classical robusticity (M3 / M1 *100)	
		Right	Left	Right	Left	Right	Left
Cro-Magnon	4297 and 4298		12.5		17.4	13.5	11.7
	4299		16		20		14.1
	4301		13.4		17.5		
MUP	Females	13.3 ± 1.5 (3)	12.6 ± 0.9 (5)	16.7 ± 3.2 (3)	15.3 ± 2.3 (5)	13 ± 1.8 (2)	13 ± 0.9 (4)
	Males	14.9 ± 1.8 (13)	14.5 ± 1.9 (16)	16.7 ± 2.8 (13)	16.3 ± 2.7 (16)	12.6 ± 1 (5)	12.1 ± 1.2 (9)
LUP	Females	14.5 ± 2.2 (6)	14.5 ± 1.7 (5)	15.1 ± 3.2 (6)	15 ± 4.2 (5)	13.9 ± 0.9 (4)	12.8 ± 0.9 (4)
	Males	14.7 ± 2.1 (12)	14.8 ± 2.5 (12)	15.4 ± 2.4 (12)	14.6 ± 2.5 (12)	13.5 ± 1.6 (12)	12.5 ± 0.7 (9)

Table 9. Radius maximum length and proximal dimensions

		Maximum Length (M1)	Head Diameter	Distal Breadth (M5(6))
Cro-Magnon	4303 (left)	267.0	25.9	
	4304 (right)	269.7		
	4305 (left)		22	
	4306 (right)	266.6		34
	4307 (left)	267.3		
MUP	Females	246.9 ± 14.3 (6)	21.7 ± 1.5 (4)	30.3 ± 1.2 (3)
	Males	268.8 ± 17.3 (13)	23.3 ± 1.7 (12)	34.6 ± 2.6 (4)
LUP	Females	214.6 ± 18.4 (7)	18.9 (1)	30.4 ± 2.7 (4)
	Males	242.3 ± 14.1 (12)	19.7 (1)	31 ± 2.2 (4)

Table 10. Radius shaft dimensions and robusticity

		Crest AP Diameter (M5)		Crest M-L Diameter (M4)		Distal Circumference (M3)		Classical robusticity	
		Right	Left	Right	Left	Right	Left	Right	Left
Cro Magnon	4303		9.8		16.9		43		16.1
	4304	13.8		18.5		46		17.1	
	4305		11.9		16.9		40		
	4306	11.6		15.7		43		16.1	
	4307		13.4		19		46		17.2
MUP	Females	11.5 ± 1.5 (4)	10.9 ± 1.2 (5)	16 ± 3 (4)	15.1 ± 2.5 (5)	39.1 ± 5.5 (4)	39 ± 2.9 (4)	14.8 ± 1.5 (3)	15.4 ± 1 (4)
	Males	12.4 ± 1.2 (13)	11.9 ± 0.8 (15)	16.4 ± 2.1 (13)	15.7 ± 1.3 (14)	41.6 ± 4.5 (13)	39.8 ± 3.4 (14)	15 ± 1.4 (9)	15 ± 0.8 (11)
LUP	Females	10.7 ± 1 (6)	9.5 ± 1 (6)	14.1 ± 2.4 (8)	13 ± 1.6 (6)	37 ± 5.5 (6)	33.9 ± 4.4 (4)	17 ± 0.9 (4)	15.3 ± 1.1 (3)
	Males	11.6 ± 1.4 (15)	11.5 ± 1.1 (11)	16.3 ± 1.5 (15)	15.3 ± 1.3 (11)	40.2 ± 2.9 (11)	40 ± 3 (12)	16.7 ± 0.8 (9)	16.1 ± 0.6 (7)

Table 11.

Associations of bones from Cro-Magnon upper limb remains in the present study and in Vallois and Billy (1965).

Present study	Bone	SV code	Vallois and Billy 1965
Alpha	Left Ulna	4299	Cro-Magnon 1
	Right clavicle	4290	Not associated with a specific individual
	Right scapula	4292	Not associated with a specific individual
	Right radius	4304	Not associated with a specific individual
Beta	Right humerus	4294	Cro-Magnon 3
	Left humerus	4295	Cro-Magnon 3
	Left ulna	4301	Cro-Magnon 2
	Left radius	4305	Not associated with a specific individual
Gamma	Left humerus	4293	Cro-Magnon 2
	Right ulna	4300	Cro-Magnon 1
	Left ulna	4302	Cro-Magnon 3
	Left radius	4303	Cro-Magnon 2
Delta	Right ulna	4297	Cro-Magnon 3
	Left ulna	4298	Cro-Magnon 2

Figures

Figure 1. Bivariate plot of humeral head anteroposterior diameter versus humeral distal minimum circumference.

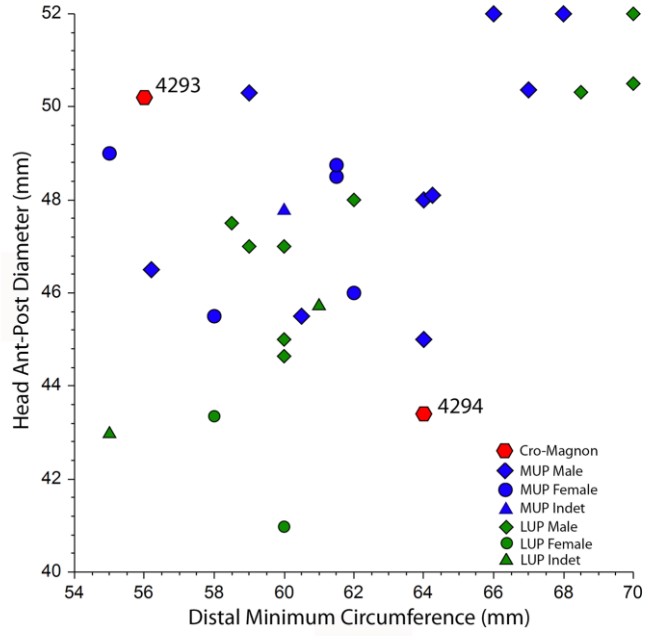

Figure 2. Bivariate plots of humeral mid-distal (35%) polar moment vs. body mass times humeral lengths. Body mass estimates are those of Gamma for 4293 and of Beta for 4294 and 4295. A) Right humeri. B) Left humeri.

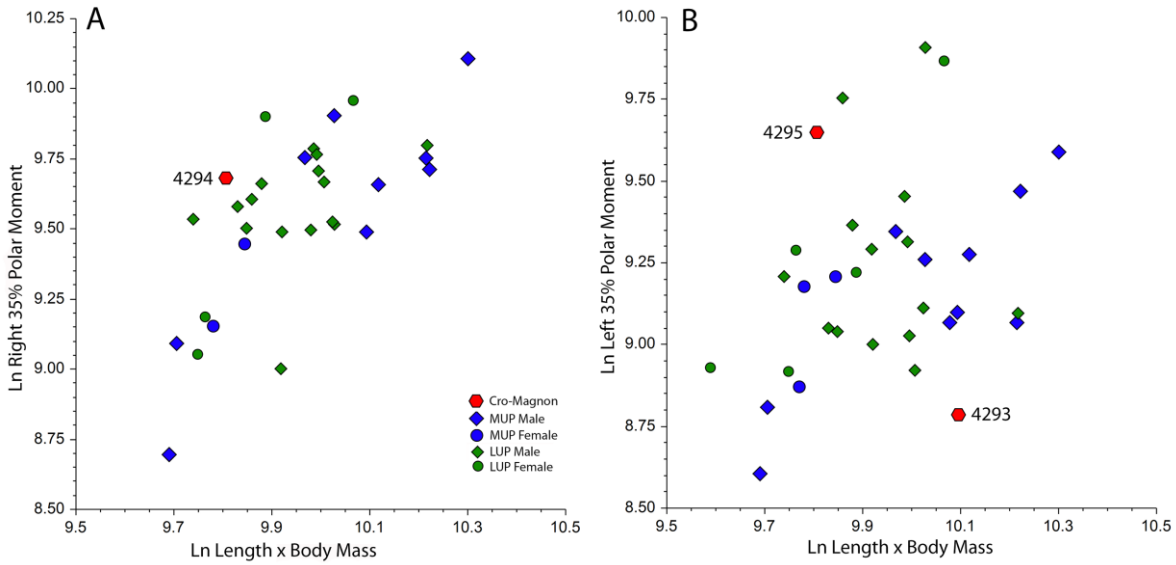

729

730

731 Figure 3. Boxplots of the Cro-Magnon (4294/95), MUP, and LUP humeral asymmetry of mid-distal
732 (35%) polar moments.

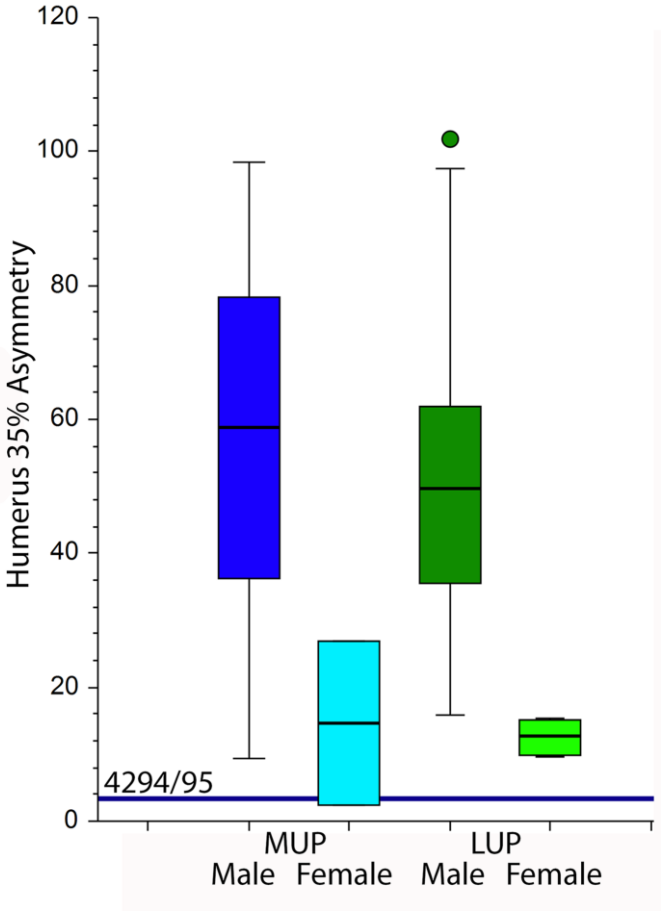

733

734

735

Figure 4. Upper limb bones allocated to Alpha in this study.

Figure 5. Upper limb bones allocated to Beta in this study.

Figure 6. Upper limb bones allocated to Gamma in this study.

Figure 7. Upper limb bones allocated to Delta in this study.

793